Zeitschrift: Schweizerische mineralogische und petrographische Mitteilungen = Bulletin suisse de minéralogie et pétrographie

Band: 80 (2000)

Heft: 1

Artikel: In-situ measurement of reaction volumes using pressure analysis

Autor: Mok, Ulrich / Girsperger, Sven

DOI: https://doi.org/10.5169/seals-60953

SCHWEIZ. MINERAL. PETROGR. MITT. 80, 85–92, 2000

In-situ measurement of reaction volumes using pressure analysis

by *Ulrich Mok*[1] and *Sven Girsperger*[2]

Abstract

We examined the feasibility and sensitivity of pressure analysis as an experimental tool to determine reaction volumes at elevated pressure and temperature. Pressure analysis is based on the following principle: a sample undergoing a volume change during a first or a second order transition in a pressurized vessel will cause a change in the confining pressure system. We show that the shape and intensity of the pressure signals can be used to study reaction equilibrium and kinetics. Moreover, recent improvements in experimental techniques have made it possible to determine in-situ volume changes of reactions. The design of the apparatus and the experimental procedure used for such analysis is outlined in this paper. We discuss the experimental procedure using several, well-studied phase transitions as examples. Experimental results for the α–β quartz transition, melting and polymorphic reactions in the CsCl system, and the NaCl–H_2O liquidus reaction up to 860 °C and 350 MPa are presented. Previous experiments were reproduced with good accuracy and some new data are generated for the CsCl system. Currently we can apply this method to kinetically fast and slow reactions with volume changes larger than 0.1–0.5%.

Keywords: experimental petrology, pressure analysis, phase transition, reaction kinetics.

Introduction

In-situ investigations of non-quenchable phase transitions at elevated pressure and temperature are most relevant in geology, geophysics and material sciences. Common in-situ techniques for a wide range of P and T conditions are thermal analysis, differential thermal analysis, calorimetry, in-situ optical and X-ray techniques, and resistivity measurements (see ULMER and BARNES, 1987, for an overview). Pressure analysis (PA) on the other hand is less commonly used. This method takes advantage of the pressure signal associated with the volume change of a sample in a fixed volume vessel, and is most useful for reversible first and second order reactions (e.g., BRIDGEMAN, 1942; FRANCK and TÖDHEIDE, 1959; KANEDA et al., 1971; MIRWALD, 1979; SCHRAMKE et al., 1982). In our laboratory, PA has been used at pressures up to 450 MPa and 1000 °C (RAZ, 1983; PHILIPP, 1988), but as of yet, the potential and limitations of this method have not been tested in full detail. PA measurements are usually conducted in temperature scans during which the sample is heated at a constant rate. The pressure and temperature signals before, during and after a phase transition are recorded and are used to determine the phase transition curve as a function of P and T. A novel experimental setup allows us to determine in-situ volume changes of reactions. To test the re-designed apparatus, we chose to examine several, previously well studied phase transitions, including the α–β quartz (e.g., CARPENTER et al., 1998), the CsCl II-I transitions (e.g., CLARK, 1959), the CsCl melting reactions (e.g., KAYLOR et al., 1960) and the liquidus reactions in the NaCl–H_2O system (e.g., BODNAR and STERNER, 1985; GUNTER et al., 1983).

The apparatus

Experiments were carried out in René 41, externally heated "cold-seal" type pressure apparatus. The vessel's length is 500 mm and its outer diameter is 50 mm. The bore is 6.5 mm wide and 450 mm deep and contains a stainless-steel filler rod that holds the sample. The sample is contained either in a welded shut gold capsule or placed into the vessel as is (e.g., quartz specimen). Argon

[1] Earth, Atmospheric, and Planetary Sciences, MIT, Cambridge, MA 02139, USA.
[2] Institut für Mineralogie und Petrographie, ETH Zürich, CH-8092 Zürich, Switzerland. <svengirs@erdw.ethz.ch>

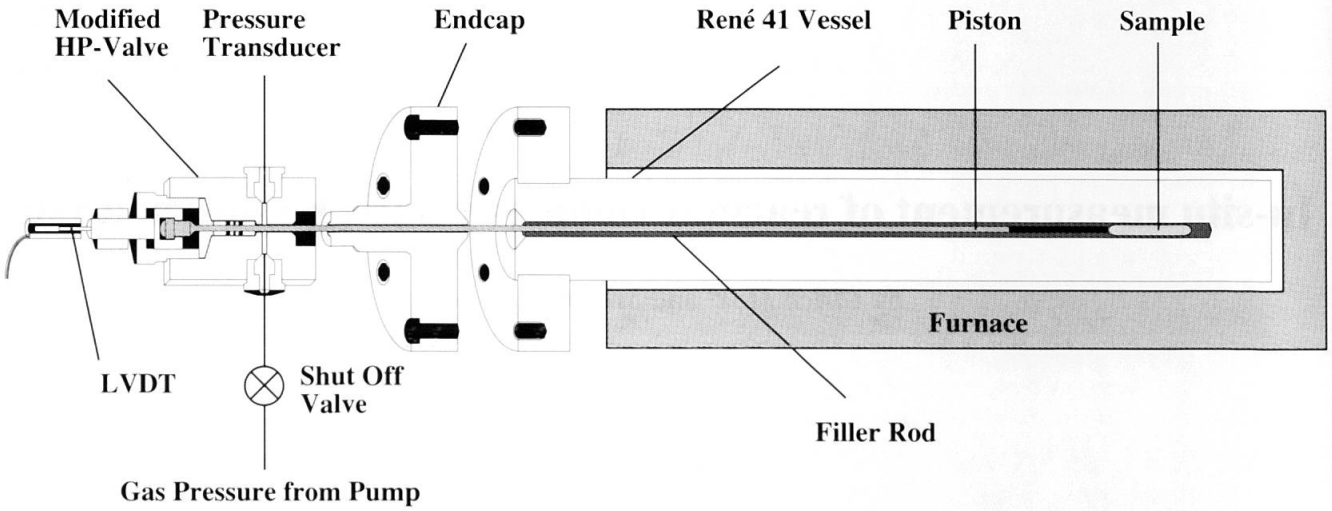

Fig. 1 Schematic layout of the externally heated pressure vessel used for quantitative pressure analysis. Vessel, endcap, and fittings are shown. The total assembly length is 750 mm. The sample is contained in a stainless-steel filler rod that fills the vessel's bore. The volume is changed by a long piston, which is attached to a high-pressure valve. The piston displacement is measured by a LVDT.

pressure is generated with an air-driven membrane pump and a water-driven intensifier (> 300 MPa). The pressure limit of the apparatus is 750 MPa. Pressure is recorded using a high-pressure transducer, which was calibrated against two Heise gages. Pressure accuracy is believed to be ± 0.5 MPa. The furnace temperature is controlled using an external type K thermocouple, a PID controller and a thyristor. A computer-controlled external DC signal is used to achieve maximum heating rates of 10 °C/min and maximum cooling rates of 2 °C/min. The vessel's length ensures a low temperature gradient of less than 1 °C (at 700 °C) across a hot spot of 30 mm. The temperature inside the autoclave is measured using a type N internal thermocouple, which was inserted into the filler rod. All thermocouples were initially calibrated against a Pt-Pt10Rh (type S) reference element, and temperature measurements are accurate to ± 2 °C after calibration. The maximum working temperature is 1000 °C (at 100 MPa).

The assembly used for quantitative volumetric measurements is shown in more detail in figure 1. The filler rod contains a long, displaceable piston (L = 400 mm, D = 3.10 mm), which is brazed to a high-pressure valve stem (D = 3.175 mm). The piston's tip is located directly near the sample to be subjected to the same temperature. The piston can be moved manually to generate a positive or negative pressure change. The according volume change can be determined by the linear displacement, which is measured with an LVDT.

The autoclave pressure, sample temperature and/or piston's displacement are measured using a 20 channel HP-3495A multiplexer and a 20 bit HP-3456A voltmeter. Voltmeter and DC sources are connected via GPIB bus to a Macintosh IIcx, which is equipped with a National Instruments GPIB interface card. The software LabView™ was used for experimental control, data storage, and data processing.

Experimental procedure and signal analysis

The sample is loaded by means of the filler rod and the vessel is slowly pressurized to experimental conditions to test for pressure leaks. The oven is set to an initial temperature 10–20 °C below the reaction temperature. After temperature and pressure equilibration, the vessel is disconnected from the pressure line to reduce the overall gas

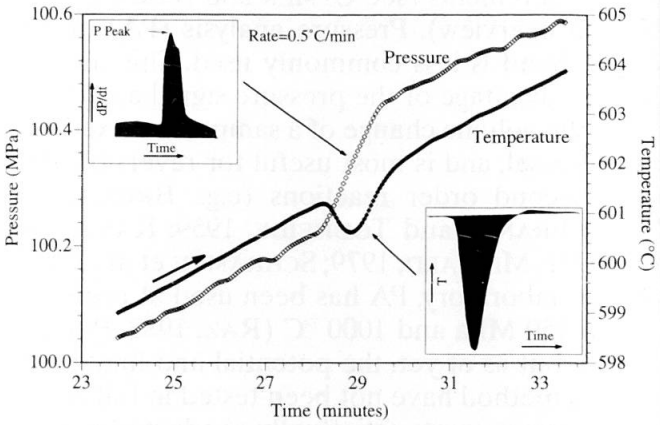

Fig. 2 Simultaneous pressure and temperature analysis of the α–β quartz transition. The reaction is endothermic and shows a positive ΔV. The differential pressure and temperature signals are shown in insets. Maximum gradients in the T and P curves occur at the same time and most likely indicate maximum reaction progress.

volume. The furnace is then heated at a constant rate 10–20 °C beyond the reaction temperature. The final temperature is maintained for approximately 1 hour until the scan is reversed and the furnace cooled down to the original settings. Internal temperature near the sample as well as pressure are recorded continuously as a function of time. An example of a simultaneous pressure and thermal analysis of the α–β quartz transition is shown in figure 2. At the transition temperature, the pressure signal shows a positive and discontinuous increase according to the positive volume change of the reaction. At the same time the sample temperature decreases due to the negative reaction enthalpy. The peak of the temperature signal and the largest gradient in the pressure signal (see inserts) match very well and indicate the point of maximum reaction progress.

More detailed examples of pressure analysis scans are shown in figures 3A–3D. Temperature was used instead of time as x-axis, so heating and cooling scans (arrows indicate the run direction) could be plotted on top of each other. No thermal analyses were conducted in these cases. Several experimental parameters can be determined from the PA runs, such as the baselines before and after the reaction, P and T of the onset (T_i) and the end of a reaction (T_f), the point of maximum reaction progress (T_P), as well as the pressure change ΔP_R. The reaction onset and the end of heating (+) and cooling (–) runs are defined by the difference between the measured signal and the extrapolated baseline (PHILIPP, 1988). In most cases, the baseline can be reasonably well approximated by a straight line for the covered temperature interval (dotted line in figures 3A, 3C, 3D). However, α-quartz shows non-linear thermal expansion below the transition temperature (e.g., RAZ, 1983), and the baseline has to be either defined by a non-linear curve, or by using points closer to the transition temperature (Fig. 3B). Pressure and temperature for the point where the reaction progress is largest are found by numerical differentiation of the pressure-time curves (see Fig. 2). The pressure change of a reaction ΔP_R is determined at the point of maximum reaction progress as the isothermal pressure difference between the two extrapolated baselines. A three-step procedure is

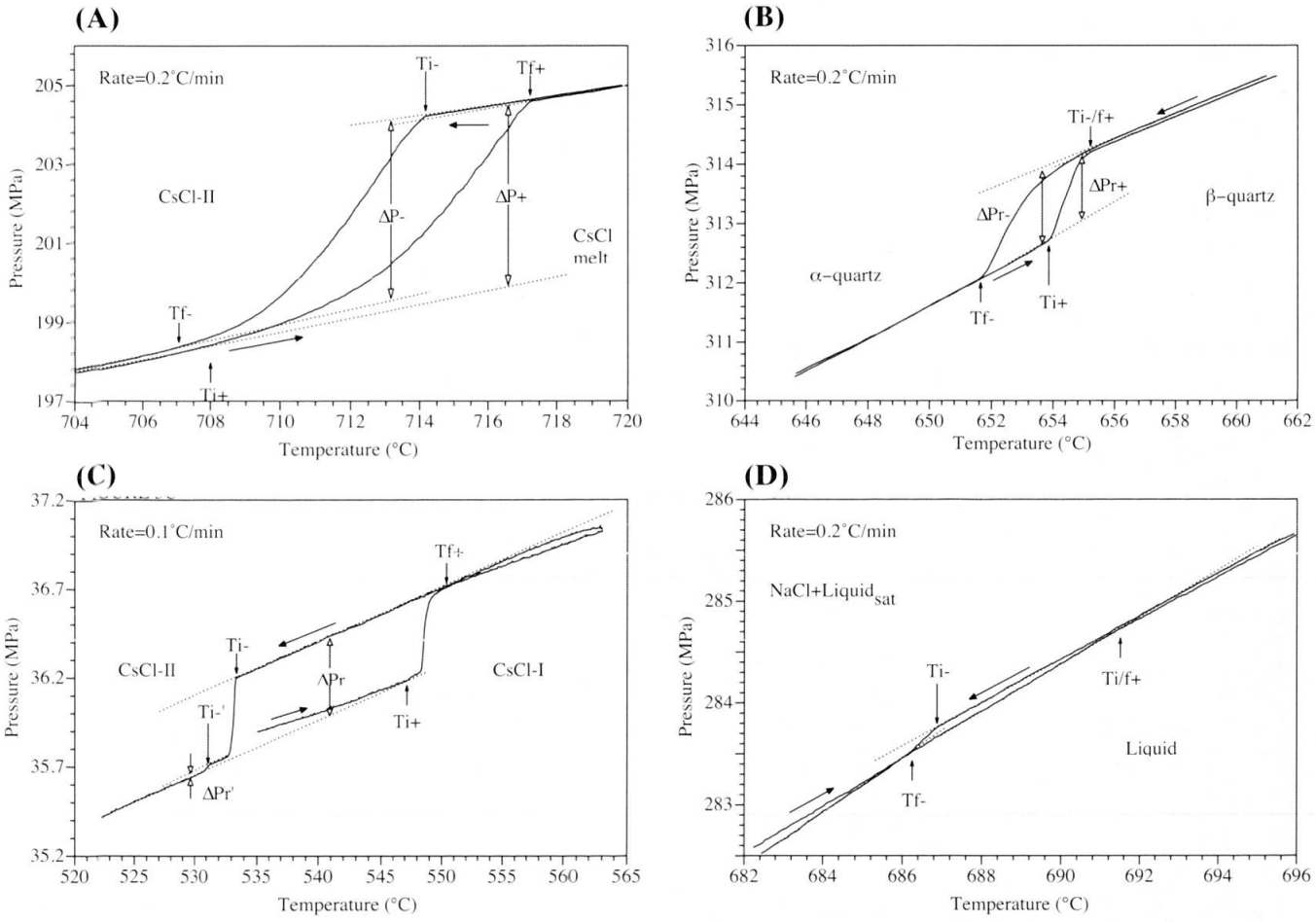

Fig. 3 Reversed pressure analysis runs of four phase transitions: (A) CsCl II-melt, (B) α-β quartz, (C) CsCl II-I, (D) NaCl-liquidus. Arrows indicate heating (+), and cooling (–) runs. Heating and cooling rates are 0.1 or 0.2 °C/min. The pressure signals show different peak characteristics depending on the type of reaction. See text for details.

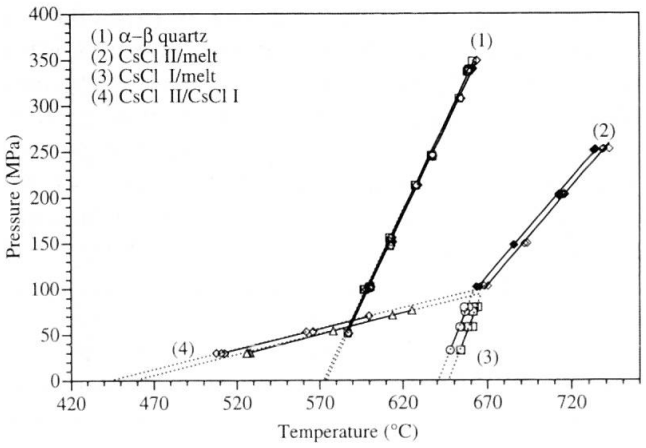

Fig. 4 Phase diagram (P-T) of the CsCl system and the α–β quartz transition up to 750 °C and 350 MPa derived from PA data. Data points for heating and cooling runs are shown separately and can be fitted by straight lines. The thermal hysteresis for the CsCl reactions is larger than for the quartz reaction. The average fit equations are listed in table 1.

used to measure in-situ volume changes of reactions:

– firstly, a pressure scan is conducted as described above and the pressure change of the reaction ΔP_R is determined.

– secondly, the system temperature is set slightly (~ 1 °C) below the onset temperature of the reaction.

– by means of the piston, the pressure is increased by ΔP_R, and the correspondent piston displacement ΔL^+ is measured.

Step two and three are repeated on the high temperature side of the transition, only that the pressure is now decreased by ΔP_R and ΔL^- is measured. The P-T conditions are identical for sample and piston, so corrections for vessel expansion or gas compressibility are not required. The molar volume change ΔV_R° is calculated by:

$$\Delta V_R^\circ = \frac{m_S}{M_S^\circ}\left(\frac{\Delta P_R}{\Delta P_S}\right)\Delta L\,\pi r^2,$$

with m_S and M_S° being the sample weight and the molar weight respectively, ΔP_S the simulated pressure change, r the radius of the piston, and ΔL the piston's displacement. For a given volume change of reaction, the magnitude of the pressure signal depends on the compressibility of the pressure medium argon and the method's sensitivity therefore increases with increasing pressure. Ideally, $\Delta P_R/\Delta P_S$ is kept close to 1 to minimize non-linearities.

Results

The pressure signals for each reaction examined are characteristic and are discussed briefly. The CsCl –> melt transition curve (Fig. 3A) shows a gradual onset on the low-temperature side with a wide melting temperature interval of about 10 °C. The pressure changes at the end of the reaction and the onset of crystallization are sharp. The difference in the baseline slope of the P-T curve before and after the reaction indicates the differences in thermal expansion and compressibility between the melt and the solid phase. It should be noted that the width of the melting signal depends on the reaction kinetics, the heating/cooling rate and the temperature gradient across the sample.

The pressure curve of the α-β quartz transition suggests a narrow reaction zone with a sharp on-

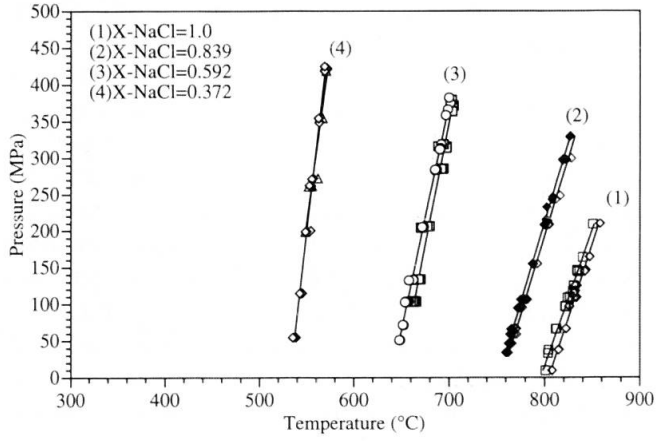

Fig. 5 Phase diagram (P-T) for the NaCl–H_2O liquidus reaction. Curves are shown for different NaCl contents (X_{NaCl} = 1 to X_{NaCl} = 0.37). The equilibrium curves of reversed PA runs (rates = 0.5–0.1 °C/min) are increasingly steeper for lower salt contents.

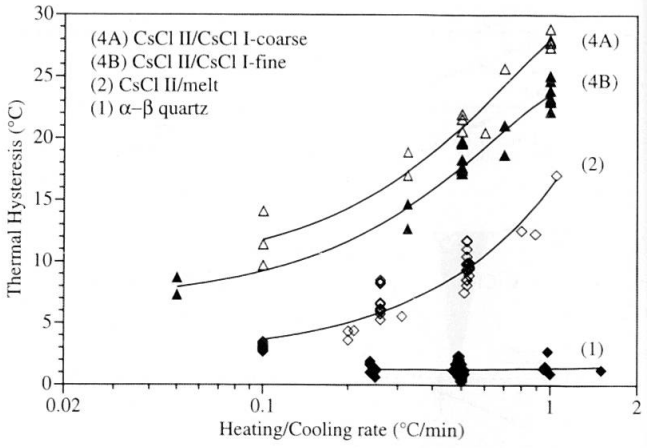

Fig. 6 Rate dependence of the thermal hysteresis of four reactions: the thermal hysteresis of the CsCl reactions shows a strong decrease with decreasing scan rates. The hysteresis of the α–β quartz reaction, on the other hand, was much smaller (1 °C) and quite insensitive for the chosen rates (see text for details).

Tab. 1 Pressure analysis data (P-T, ΔV_R, ΔT_H) of the examined reactions in comparison to literature data (in quotes)

Reaction	**T =**	***dT/dP***	ΔV_R **(cc/mol)**		ΔS_R (J/mol/K)		ΔT_H	
α–β quartz	**573.3 + 25.8E-2(P)**	*(25.8E-2[1])*	**0.115***	*(0.118[2])*	0.446	*(0.462[9])*	**1–2**	*(1.4[2])*
CsCl II/melt	**620.0 + 46.4E-2(P)**	*(48.3E-2[3])*	**9.7****	*(10[3])*	20.9	*(20.9[3])*	**1–3**	
CsCl I/mel	**644.8 + 19.5E-2(P)**	*(20.3E-2[4,5])*	**3.9***	*(3.0[3])*	20.0	*(17[3])*		
CsCl II/CsCl I	**454.2 + 21.9E-1(P)**	*(20E-1[3])*	**7.6***	*(8[6])*	3.47	*(3.94[3])*	**6–10**	*(45[10])*
NaCl/melt	**800.1 + 26.0E-2(P)**	*(24.2E-2[7])*	**5.8**	*(7.55[8])*	24.0	*(26.2[9])*		

Temperature (T) in °C, pressure (P) in MPa
* at 1 bar; ** at 99.5 MPa, 665 °C
[1]COE and PATTERSON (1969), [2]GHAZI (1985), [3]CLARK (1959), [4]KAYLOR et al. (1960), [5]MARCHIDAN and PANDELE (1975), [6]JOHNSON et al. (1955), [7]CHOU (1982), [8]SCHINKE and SAUERWALD (1956), [9]RAZ (1983), [10]RAO and RAO (1966)

set at the low-T side (Fig. 3B). The cooling signal is always much broader, most likely due to the occurrence of an intermediate incommensurate phase (e.g., BACHHEIMER, 1980). Again, the baseline slopes before and after the reaction differ significantly, in this specific case somewhat complicated by the nonlinear thermal expansion of the α-phase close to the reaction temperature.

The CsCl II-I solid transition (Fig. 3C) is known to be very fast because of the structural similarity of the two phases. The diffusionless, deviatoric-dominant reaction has a large volume change of 17% resulting in a large PA signal even at low system pressures. The P-T curve indicates a sharp onset (T_f, T_i) and the reaction completes in an extremely narrow temperature interval. The baseline slopes of the low and high temperature phase are very similar. Frequently a satellite peak appears during the cooling reaction ($\Delta P_r'$), which varies in height and occurrence. We interpret this phenomenon to be most likely the result of an initial fast "de-pressurization" of the system, which moves the overall P-T conditions away from equilibrium. Note that, for a positive dP/dT of reaction, subsequent cooling is necessary to complete the reaction.

The NaCl–H_2O liquidus reaction (Fig. 3D) is not defined by a distinct volume change, but rather by a discontinuity in the heating signal. The discontinuity is caused by the difference in thermal expansion and compressibility of the undersaturated salt-water solution on one side and the NaCl crystal + saturated solution on the other side. The cooling signal shows a small peak at T_i-/T_f-, most likely due to supercooling. Currently the resolution of the apparatus allows us to measure the NaCl–H_2O liquidus reactions at salt contents as low as $X_{NaCl} = 0.37$ (MOK, 1993).

Phase diagrams up to 450 MPa and 850 °C for the NaCl –> melt, the CsCl reactions and the α-β quartz transition were constructed on the basis of repeated experiments as illustrated in figures 4 and 5. The fitted curves and the P-T slopes for the examined reactions agree very well with literature data (see Tab. 1).

To further elaborate the use of pressure analysis we examined the thermal hysteresis of the individual reactions. We define the thermal hysteresis ΔT_H here as the isobaric temperature difference between the points of maximum reaction progress (T_P) of heating and cooling runs. Thermal hysteresis is a function of experimental constraints such as scan rate and temperature gradient over the sample, as well as reaction-dependent parameters, such as reaction kinetics, occurrence of an intermediate phase (e.g., incommensurate quartz), and volume change of the reaction. Several authors (e.g., RAO and RAO, 1966 and 1975; KABBANY et al., 1986) pointed out that the thermal hysteresis is also a function of additional free energy contributions from surface area, strain energy, as well as crystal defects. To distinguish such phase property contributions to hysteresis from transient processes (e.g., heat flow during heating or cooling, dissipation of reaction enthalpy) it is necessary to determine ΔT_H at "zero rate". In practice, experiments conducted at small scan rates can be used to extrapolate ΔT_H to zero rates more reliably. Such studies are particularly important for bracketing the thermodynamic equilibrium of reactions. PA is especially suitable to examine thermal hysteresis at small scan rates, because the system pressure can be conserved over time and is not subjected to diffusion such as a heat.

The thermal hysteresis of the CsCl reactions and the α–β quartz transition as a function of the heating/cooling rate is plotted in figure 6. The scan rates are between 0.05 °C/min and 1.5 °C/min. The α–β quartz transition shows no change in hysteresis at the given rates and the average ΔT_H is 1.4 °C. In good agreement with this finding, GHAZI et al.

(1985) reported 1 °C at a rate of 0.02 °C/min at 1 bar. The hysteresis of the CsCl II-melt (< 3 °C at low rates) and the CsCl II-I reactions on the other hand are strongly rate dependent and ΔT_H is largest for the CsCl II-I transition (Tab. 1). Two sets of CsCl II-I experiments are shown. Initially, PA runs at different scan rates were conducted using a fine-grained CsCl powder. After the experiments, the sample was brought above the CsCl melting point and subsequently slowly cooled with the intention of creating an annealed sample with coarse grain size. The experiments were then repeated. The coarse-grained sample shows a finite hysteresis of about 10 °C. The rate dependence of ΔT_H of the fine-grained sample is parallel to the coarse grained sample, but the hysteresis at a given rate is about 2 °C smaller and the transition suggests a finite hysteresis of 6–10 °C.

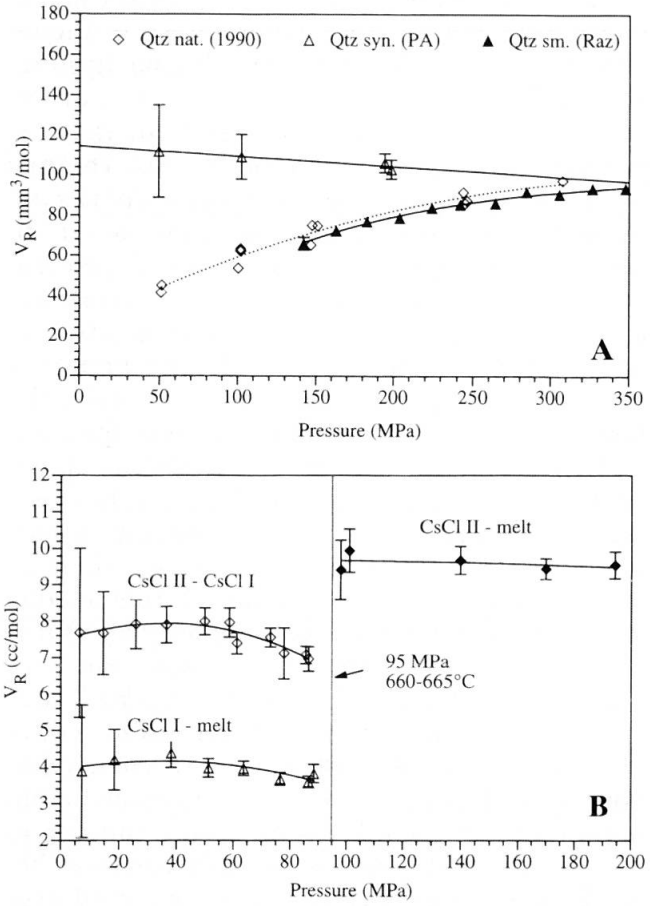

Fig. 7 (A) In-situ molar volume change of the quartz transition up to 350 MPa. This test was conducted to validate the newly designed quantitative PA setup. Former erroneous data is shown for comparison. The error bars indicate the maximum absolute error. The reproducibility of the data is much better and the average data agrees well with literature (see Tab. 1).
(B) Molar volume changes in the CsCl system determined by PA. Three reactions are shown together as a function of the equilibrium pressure. See text for details.

Both sets of experiments were otherwise conducted at identical conditions and illustrate the influence of additional surface energy and potential crystal defects on ΔT_H. The temperature difference in hysteresis of 2 °C for the CsCl II-I transition is equivalent to a free energy contribution of 6.6 J/mol introduced during grinding the sample (thermodynamic data from KAYLOR, 1960, and MARCHIDAN and PANDELE, 1975). However, more detailed experiments including microstructural examinations are necessary to further examine the relationship between hysteresis and grain size.

Quantitative in-situ measurement of volume changes ΔV_R was performed for the α–β quartz transition first. Three sets of data are plotted in figure 7A. The recent PA data are shown with error bars as an estimate of the absolute error of the measurement. Two previous PA tests were conducted with the displaceable piston outside the hot spot of the vessel (at room temperature) and are plotted for two reasons. Firstly, the data shows that the reproducibility of PA measurements is much better than the absolute measurement error. Secondly, the previous data show an erroneous decrease in ΔV_R towards lower pressure, suggesting that the piston's displacement has to occur at sample temperature to obtain accurate values for ΔV_R. The heating and cooling runs of the PA data at 500, 1000, and 2000 bar pressure give ΔV_R between 0.11 and 0.10 cc/mol with highest values for the low pressure experiment. A straight fit line yields a ΔV_R of 0.11 ± 0.01 cc/mol at ambient pressure, which agrees very well with previous experiments conducted by SHAPIRO and CUMMINS (1968) and HÖCHLI (1970) ($\Delta V_R = 0.11$ cc/mol). More recent dilatometry measurements conducted by GHAZI, 1985 (0.118 cc/mol) and RAZ, 1983 (0.11 cc/mol) confirm the volumetric PA data.

New data were generated for the CsCl system (Fig. 7B). The molar volume changes ΔV_R of the three CsCl transitions at different temperatures are plotted as a function of the reaction pressure. A dashed line indicates the triple point of the system at 95 MPa and 660–665 °C (Fig. 4). On the low-pressure side, the II-I transition suggests a ΔV_R of 7.6-8 cc/mol up to about 60 MPa (7.6 cc/mol is the extrapolated value at ambient pressure). The equivalent ΔV_R for the CsCl I-melt reaction is much smaller (3.9 cc/mol at 0.1 MPa). Our data seems to suggest a pressure dependence of the volume change. Especially for the I-II transition, ΔV_R towards the triple point are measured to be significantly lower (ΔV_R (I-II): 6.5 cc/mol, ΔV_R (I-melt): 3.5 cc/mol). On the high-pressure side ΔV_R for the II-melt reaction is highest (9.7 cc/mol at 95 MPa). For the volumetric data to

be internally consistent it is required that the extrapolated values for ΔV_R add up at the triple point, i.e.: ΔV_R *(I–II)* + ΔV_R *(I-melt)* = ΔV_R *(II-melt)*. Within the given uncertainties, this relationship is confirmed when the extrapolated data is used. Using the Clausius-Clapeyron relation $dP/dT = \Delta S_R/\Delta V_R$, we also calculated the entropy change of the reaction ΔS_R and compared them to literature (Tab. 1). To our knowledge these data represent the first in-situ measurements of ΔV_R of the CsCl melting reactions.

Conclusions

Several fast and reversible phase transitions have been presented to illustrate the feasibility and the range of possible applications of pressure analysis. The purpose of this paper is to show the wealth of interesting details with respect to phase equilibrium, kinetics, phase diagram, and volumetric data that this in-situ method can provide. In part, such data can only be obtained by more sophisticated methods (i.e., in-situ X-ray studies), or not at all up to this point (i.e., in-situ volume changes of melting reactions). The data generated during this study are generally in agreement with literature and suggest that PA can be used to derive quantitative data on phase transitions. Pressure analysis is a highly sensitive method and there is room for apparative improvements and adaptations depending on the nature of the reaction to be studied. Some possible improvements to the current experimental setup shall be mentioned here in the order of descending effectiveness:

– Further reduction of vessel dead volume. Theoretically, if the dead volume is approaching ΔV_R, the sensitivity of the method will rise towards infinity.

– Control of room temperature to increase the method's resolution for slow reactions with small ΔV_R. Such reactions require run times of several days or weeks. Pressure fluctuations due to temperature changes in a non-controlled environment may decrease the transient resolution of PA.

– The installation of an automated volumetric control (e.g., stepping motor) will allow isobaric experiments to be run and direct measurement of ΔV_R. Pressure analysis can then be used for kinetic studies, which require constant P and T conditions.

– Apparative improvements (e.g., the use of a higher resolution pressure transducer).

Acknowledgements

The experiments were conducted during a Ph. D. Thesis at the *Institut für Mineralogie und Petrographie, ETH Zürich*. The work was supported by grants from the *Schweizerischer Nationalfonds* (#20-26223.89, #20-30768.91).

Appendix

MATERIALS

Quartz: a single synthetic quartz crystal (clear and free of inclusions) was cut into a small cylinder of 36 mm length and 5.36 mm diameter. Sample weight was 2.15378 g.

CsCl: coarse-grained CsCl (puriss. p.a.; Fluka Chemicals) was dried for 48 hours at 120 °C. An aliquot was used as is for phase diagram and volumetric studies (m = 0.653 g). A second sample (m = 0.371 g) was used for the hysteresis study and was crushed in a mortar to reduce the original grain size to less than 50 µm. Each sample was filled into a 30 mm long gold capsule and welded shut with a plasma arc.

NaCl–H_2O: for the NaCl melting reaction, NaCl (suprapure, MERCK Chemicals) was dried and filled into a 20 mm long gold capsule. Longer capsules (50 mm) were used for the NaCl liquidus samples. HPLC grade water was added (by weight) to obtain different salt-water compositions. The water-salt mixtures were frozen with liquid nitrogen during welding.

References

BACHHEIMER, J.P. (1980): An anomaly in the β phase near the α–β phase transition of quartz. J. Phys. Lett., 41L, 559–561.

BRIDGEMAN, P.W. (1942): Pressure-volume relations for seventeen elements to 100.00 kg/cm². Proc. Amer. Acad. Arts Sci., 74, 425–440.

BODNAR, R.J. and STERNER, S.M. (1985): Synthetic fluid inclusions in natural quartz III: Determination of phase equilibrium properties in the system H_2O–NaCl to 1000 °C and 1500 bars. Geochim. Cosmochim. Acta, 49, 1985, 1861–1873.

GUNTER, W.D., I-MING CHOU and GIRSPERGER, S. (1983): Phase relations in the system NaCl–KCl–H_2O II: Differential thermal analysis of the halite liquidus in the NaCl–H_2O binary system above 450 °C. Geochim. Cosmochim. Acta, 47, 863–873.

CLARK, S.P. (1959): Effect of Pressure on the Melting Points of Eight Alkali Halides. J. Chem. Phys. 31, 1526–1531.

CARPENTER, M.A., SALJE, E.K.H., GRAEME-BARBER, A., WRUCK, B., DOVE, M.T. and KNIGHT, K.S. (1998): Calibration of excess thermodynamic properties and elastic constant variations associated with the α–β transition in quartz. Amer. Mineralogist, 83, 2–22.

COE, R.S., PATERSON, M.S. (1969): The α–β Inversion in Quartz: A Coherent Phase Transition under Nonhydrostatic Stress. J. Geoph. Res., 74:20, 4921–4948.

FRANCK, E.U. and TÖDHEIDE, K. (1959): Thermische Eigenschaften überkritischer Mischungen von Kohlendioxid und Wasser bis zu 750 °C und 2000 Atm. Zeitschrift für Physikalische Chemie – Neue Folge, 22, 232–245.

GHAZI, F. (1985): Contribution à L'Etude des Transitions de Phases du Quartz par Mesures de Dilatation Thermique et de Birefringence. Thèse de l'Université Scientifique et Médiale de Grenoble, 107 pp.

HÖCHLI, U.T. (1970): Ultrasonic Investigations of the First-Order α–β Phase Transition of Quartz. Solid State Commun., 8, 1487–1490.

JOHNSON, J.W., AGRON, P.A. and BREDIG, M.A. (1955): Molar Volume and Structure of Solid and Molten Cesium Halides. J. Amer. Chem. Soc., 77, 2734–2737.

KABBANY, F.EL., BADR, Y., SAID, G., TAHA, S. and MAHROUS, S. (1986): A Study of the Thermal Hysteresis in $AgNO_3$. Phys. Stat. Sol., 95a, 127–134.

KANEDA, R., YAMAMOTO, S. and NISHIBATA, K. (1971): Fixed Points of the High Pressure Scale Identified by Phase transitions in Ammonium Fluoride. In: LLOYD, E.C. (ed.): Accurate Characterisation of the High-Pressure Environment, NBS Spec. Pub. 326, 343 pp.

KAYLOR, C.E., WALDEN, G.E. and SMITH, D.F. (1960): High-Temperature Heat Content and Entropies of Cesium Cloride and Cesium Iodide. J. Phys. Chem. 64, 276–278.

MARCHIDAN, D.I. and PANDELE, L. (1975): Thermal Properties of KCl, CsCl, and Binary Mixture KCl + CsCl, High-Temperature Heat Content. Rev. Roum. Chim., 20, 229–304.

MIRWALD, P.W. (1977): Determination of Melting entropy by the Measurement of the Volume Change of Melting at High Pressure. From: High Pressure Science & Technology (1979), Vol. I, Edts.: Timmerhaus & Barber, 361–367.

MOK, U. (1993): Volumetric Determinations in the Systems NaCl–H_2O and KCl–H_2O to 450 MPa and 900 °C. Diss. ETH No. 10133, 100 pp.

PHILIPP, R.W. (1988): Phasenbeziehungen im System MgO–H_2O–CO_2–NaCl. Diss. ETH Nr. 8641, 185 Seiten.

RAO, C.N.R. and RAO, K.J. (1966): Crystal Structure Transformation of Alkali Sulphates, Nitrates and related Substances: Thermal Hysteresis in reversible transformations. J. Mat. Science 1, 238–248.

RAO, C.N.R. and RAO, K.J. (1978): Phase Transitions in Solid: An Approach to the study of the Chemistry and Physics of Solids. McGraw-Hill, New York, 330 pp.

RAZ, U. (1983): Thermal and Volumetric Measurements on Quartz and other Substances at Pressures up to 6 kbars and Temperatures up to 700 °C. Diss. ETH No. 7386, 91 pp.

SCHINKE, H. and SAUERWALD, F. (1956): Dichtemessungen XVIII. Über die Volumenänderung beim Schmelzen und den Schmelzprozess bei Salzen. Z. Anorg. Allg. Chemie, 287, 313–324.

SCHRAMKE, J.A., KERICK, D.M. and BLENCOE, J.G. (1982): Experimental Determination of the Brucite = Periclase + Water Equilibrium with a new Volumetric Technique. Amer. Mineralogist, 67, 379–399.

SHAPIRO, S.M. and CUMMINS, H.Z. (1968): Critical opalescence in quartz. Phys. Rev. Letters, 21, 1578 ff.

ULMER and BARNES, Eds (1987): Hydrothermal experimental Techniques, John Wiley & Sons, New York, 523 pp.

Manuscript received July 22, 1999; accepted November 11, 1999.